Chapter 3

Super-Speeding Jets in MHD Couette Flow

Krzysztof Mizerski

Additional information is available at the end of the chapter

http://dx.doi.org/10.5772/intechopen.79005

Abstract

A magnetohydrodynamic flow of a viscous and conducting fluid confined between two parallel differentially moving boundaries is considered. The whole system is in a *strong* magnetic field chosen in such a way that the Hartmann boundary layers which form in this problem become singular at the points where the magnetic field becomes tangent to the boundary. Two geometries are taken into account: *plane* and *spherical*. Within the class of such configurations, the velocity field of the fluid and the influence of the conductivity of the boundaries on the fluid's motion are reviewed here. In the region of singularity, where the magnetic field is tangent to the boundary, the fluid's velocity exceeds that of the moving boundary. The effect of nonzero conductivity of the boundaries on the super-speeding jets is vital and has been enlightened in a series of papers, including experimental and theoretical findings. The mechanism of the formation of super-speeding jets in the considered configurations has been explained, which is based on strong Hartmann currents allowed to enter the boundary layer due to the singularity. In the case of both perfectly conducting boundaries, the super velocity was shown to be as strong as to scale with the Hartmann number as $\mathcal{O}\left(M^{1/2}\right)$.

Keywords: super rotation, magnetohydrodynamics, MHD boundary layers, Hartmann layer singularity, nonzero conductivity

1. Introduction

Super-speeding jets in the geometry of magnetohydrodynamic (MHD) spherical Couette flow have been first noticed in the numerical simulations of Dormy et al. [1]. They have analyzed a flow of an electrically conducting fluid in a spherical gap between concentric spherical shells, rapidly and differentially rotating about a common axis in a centered axial dipolar magnetic field. The solid inner sphere, which had the same conductivity as the fluid, was spinning slightly faster than the insulating outer shell. The stationary flow obtained via DNS exhibited

a super-rotating structure near the region, where the critical magnetic field line, henceforth denoted by $\mathcal{C}$, was tangent to the outer shell. The angular velocity of the flow in that region was about 50% greater than that of the inner sphere, which was driving the flow.

Hollerbach [2] for the first time investigated numerically the effect of nonzero conductivity of the outer shell in the same spherical geometry but the outer boundary was held motionless, thus eliminating the Coriolis force from the problem. He reported that the super rotation in the singular region was greatly enhanced and scaled with the value of the Hartmann number M.[1] Hollerbach [3] studied the MHD spherical Couette flow for several different topologies of the external field lines and also observed that singular points of isolated contact of the magnetic lines with boundaries result in the formation of jets.

In a following sequence of three theoretical papers, the mechanism of super-velocity formation and the effect of nonzero conductivity of the boundaries have been explained. Dormy et al. [4] performed a joint analytical and numerical study of the system analyzed previously by Hollerbach [2], where they have described the super rotating shear layer along the critical magnetic line $\mathcal{C}$ which grazes the outer boundary and found analytic expressions for super rotation within the scope of asymptotic theory for $M \gg 1$, confirmed by the results of numerical simulations. Not only they have explained the physics of the mechanism behind the formation of super-speeding jets in the studied configuration, which relies on the enhancement of the Lorentz force accelerating the flow, due to strong currents entering the singular Hartmann boundary layer at the outer shell near the point of contact of the critical field line $\mathcal{C}$ with the boundary, but also their analysis set grounds for the following theoretical findings. The study of Mizerski and Bajer [5] greatly relied on that of Dormy et al. [4], although it involved geometries—planar and spherical, and the resting boundary was weakly conducting (as opposed to the previous study, where it was insulating). The two geometries studied by Mizerski and Bajer [5] are depicted on **Figure 1**. In the plane geometry, the bottom boundary is moving at a constant speed and has the same conductivity as the fluid, whereas the conductivity of the upper boundary relative to the fluid's conductivity ϵ is assumed small at the order $\epsilon \sim M^{-1}$. The rest of the space was an insulator. The crucial features of the external field in this configuration are that it is potential and that there exists a critical magnetic line, which grazes the upper boundary thus creating a singularity of the Hartmann layer. The two configurations depicted on **Figure 1** are planar and spherical counterparts, equivalent from the point of view of physics of the super-speeding jets which form near the singularities. The plane configuration, however, captures all the necessary physical ingredients of the problem but at the same time makes the problem more transparent, avoiding the complications resulting from the curvature of the boundaries. Mizerski and Bajer [5] utilized this simplification and demonstrated the super-velocity excess, that is, the difference between the super velocity in the cases of a conducting and insulating outer boundary scales like $\mathcal{O}\left(\varepsilon M^{3/4}\right)$. They have also studied a somewhat similar case of a strongly conducting, but thin outer shell, with conductivity being the same as that of the fluid, but the relative thickness of the conducting shell to the thickness

[1] He fitted an exponent of $M^{0.6}$ to his numerical results, which however, was later shown not to be the true asymptotic scaling law.

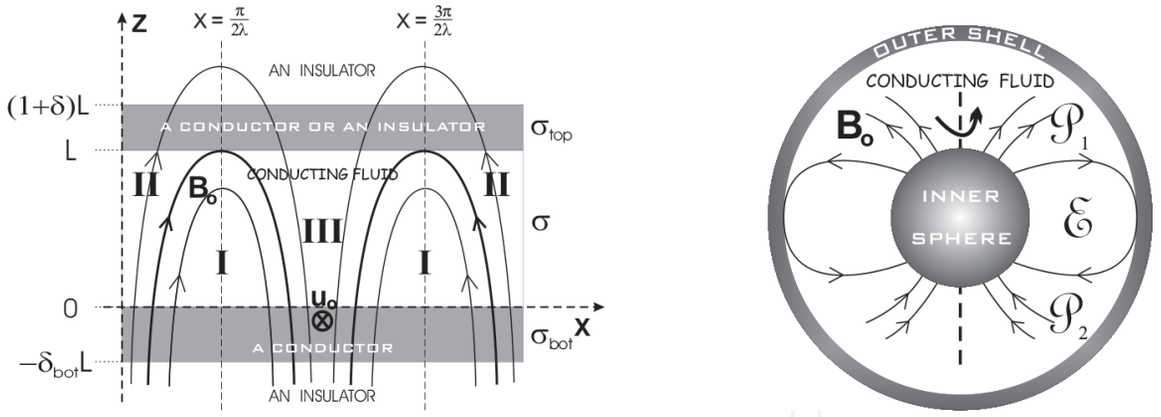

Figure 1. A sketch of the two situations considered: the plane case on the left (the bottom boundary is moving) and the spherical case on the right (the inner sphere is rotating). After Mizerski and Bajer [5].

of the fluid layer δ was assumed small, at the order $\delta \sim M^{-1}$. They demonstrated that both cases, $\epsilon \sim M^1$, $\delta \sim 1$ and the other one $\epsilon \sim 1$ and $\delta \sim M^{-1}$, are exactly equivalent in terms of the flow structure and the super-velocity magnitude. In the latter case, the super-velocity excess was shown to scale like $\mathcal{O}\left(\delta M^{3/4}\right)$. The same scalings were shown to pertain to the spherical geometry. The most notable contribution to the problem of super-speeding jets was the remarkable comprehensive analysis of Soward and Dormy [6] in the spherical geometry. They have emphasized the role of the parameter $\epsilon M^{3/4}$ (or $\delta M^{3/4}$ for the case of thin outer shell), identified in Mizerski and Bajer [5], for the general case of continuously varying relative conductivity of the outer shell ϵ from zero to infinity. They have reported the following scaling laws for the super velocity (angular velocity) in the singular region, for the case of perfectly conducting inner boundary.

$$\begin{aligned} \Omega_{max} &= \mathcal{O}\left(M^{1/2}\right) \quad \text{for} \quad 1 \ll \epsilon \ll \epsilon M^{3/4} \\ \Omega_{max} &= \mathcal{O}\left(\varepsilon^{2/3} M^{1/2}\right) \quad \text{for} \quad \epsilon \ll 1 \ll \epsilon M^{3/4} \\ \Omega_{max} &= \mathcal{O}(1) \quad \text{for} \quad \epsilon \ll \epsilon M^{3/4} \ll 1 \end{aligned} \tag{1}$$

The magnitude of the super rotation Ω_{max} was shown to be proportional to the magnitude of current on the critical $\mathcal{C}$-line, denoted by $\mathcal{J}_c$, i.e., $\Omega_{max} \sim \mathcal{J}_c$.

The phenomenon of super rotation was also observed in the experimental setup called "Derviche Tourneur Sodium" (DTS) located in Grenoble at the Université Joseph-Fourier. Nataf et al. [7] conducted experiments on the spherical Couette flow of liquid sodium in an external, centered axial dipolar field, with both boundaries differentially rotating. The outer shell was only 5 mm thick, about 27 times thinner than the fluid gap and about 8 times less electrically conductive than liquid sodium. The Hartmann number in the experiment was at the order of a thousand. They observed the super-rotating jets and obtained a very good agreement with the numerical models. However, they also observed that the super-speeding jets can be destabilized and reported oscillatory motion near the singular region. More recently, Brito et al. [8] further exploited the same DTS experimental setup and explored the effects of strong

inertia. They also reported strong super rotation; however, they clearly demonstrated that the Coriolis force tends to suppress the super-speeding jets.

Wei and Hollerbach [9] investigated numerically the effect of strong inertia, that is, large Reynolds number, on the spherical Couette flow configuration with the outer shell stationary. Three configurations of the external magnetic field were chosen, which resulted from a combination of dipolar and axial fields. The super-speeding jets have been destabilized by increasing the Reynolds number, whereas strengthening the filed had the opposite effect. Most recently, Hollerbach and Hulot [10] performed numerical analysis of a similar problem in cylindrical geometry, putting an emphasis on the role of conductivity of the boundaries. The field configurations were also chosen so as to create singularities in the flow. When the boundaries were electrically conducting, super-speeding jets were reported on the contrary to the case with insulating boundaries, when simply shear layers were observed in the singular regions. A curious observation is made by the introduction of a nonzero azimuthal component of the external field in which case the conductivity of the boundaries has the opposite effect to the previous case, greatly suppressing the magnitude of super rotation.

The motivation for some of the aforementioned studies was justified on geophysical grounds. The investigations of the Earth's interior reveal differential rotation of the inner core (cf. [11, 12]) and that the electrical conductivity of the lower mantle is nonnegligible [13]. Moreover, some evidence can be found for the existence of a very thin layer of anomalously high conductivity at the base of the mantle [14, 15]. It must be said, however, that the model of MHD spherical Couette flow is so idealized with respect to the true dynamics of the core, neglecting thermal and compositional driving, turbulence, the solidification processes at the inner core, etc., that no direct comparisons with the flow at the core-mantle boundary can be made. Nevertheless, it might be possible that the effect of super rotation manifests itself on the field zero isolines locally at the core mantle boundary.

1.1. Ferraro's law of isorotation

Throughout this chapter, we will assume that the Hartmann number,

$$M = \frac{B_0 L}{\sqrt{\mu_0 \rho \nu \eta}} = \sqrt{\frac{\sigma}{\rho \nu}} B_0 L \gg 1 \tag{2}$$

is large. In the above, μ_0, ρ, ν, η, and σ are the magnetic permeability, constant density, viscosity, magnetic diffusivity, and electrical conductivity of the fluid, respectively; B_0 is the typical strength of the external magnetic field; and L is the distance between the boundaries.

In such a case, the Ferraro's law of isorotation states that for a steady azimuthal motion about an axis of symmetry of an electrically conducting fluid, the magnitude of the angular velocity is predominantly constant along a magnetic field line. This means that in the studied configurations presented in **Figure 1**, the flow in the equatorial region $\mathscr{E}$ in the spherical case and region **I** in the planar case both bounded by the critical line which grazes the outer/upper boundary must significantly differ from the flow outside those regions. The magnetic lines

http://dx.doi.org/10.5772/intechopen.79005

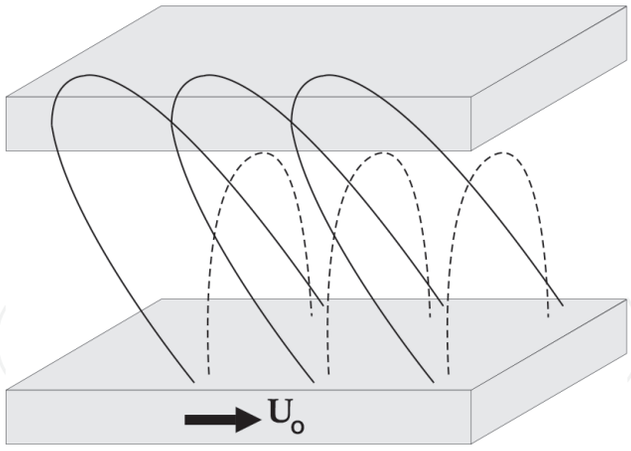

Figure 2. The moving electrically conducting boundary drags the field lines with it, but only those lines which experience drag from the top, stationary boundary are tilted (solid lines). The lines within the arcade bounded by the critical $\mathcal{C}$-line are carried with the same velocity as that of the bottom boundary. After Mizerski and Bajer [5].

within the regions $\mathscr{E}$ and **I** do not reach the outer/upper boundary and their both footpoints lie on the inner/bottom boundary, which is moving. Since the moving boundary is assumed electrically conducting with the same conductivity as the fluid, the magnetic field lines within the arcade bounded by the $\mathcal{C}$-line are carried by the fluid without any tilt. Therefore, by the Ferraro's law, the flow within the arcade must be uniform, with the same magnitude as the velocity of the moving boundary. On the contrary, the magnetic lines outside those regions extend from one boundary to the other; therefore, they are tilted due to advection by the inner/bottom boundary and the drag they experience from the outer/top, stationary boundary. The effect of competition of the moving and the stationary boundary makes the flow vary from one field line to the other. This is illustrated in **Figure 2** for the case of planar geometry.

In the following, we review the analytic approach and most important results for the two cases introduced in **Figure 1**.

2. Mathematical formulation

We study two types of stationary, magnetohydrodynamic Couette flow, that is, a flow between two parallel boundaries one of which is moving with a constant velocity: plane and spherical. The flow interacts with a strong (large Hartmann numbers) force-free magnetic field tangent to the boundaries at some isolated points. In the spherical case, the external field is a dipole field with a source at the center of the system and in the plane case, it is harmonic with oscillatory dependence in the direction perpendicular to the velocity of the moving boundary with an arbitrary period $\frac{2\pi}{k}$. **Figure 1** illustrates both the spherical and the plane cases.

We focus here on the phenomenon of super velocities in the regions of singularity of the Hartmann boundary layers which are present in this problem, that is, in the vicinity of points, where the magnetic field becomes tangent to the stationary boundary. In those regions, the fluid's velocity exceeds the velocity of the moving boundary. The aim of this chapter is to

review the influence of conductivity of the upper/outer boundary on the enhancement of the super-velocity magnitude and explain why the super velocities are larger in the case when the stationary boundary is conducting when compared to the case where it is insulating. As mentioned in the introduction, this fact was proved numerically by several authors. We adopt here the analytic approach and notations of Dormy et al. [4] and Mizerski and Bajer [5]. Majority of the analysis will be done in the simpler and therefore more transparent planar geometry.

We consider here a stationary state in which the velocity of the fluid and the induced magnetic field have only one component, the same as the velocity of the moving boundary, axisymmetric for the spherical case and translationally invariant in the direction of the flow for the flat case. Small differential rotation/motion of the boundaries is assumed for the Couette flow dominated by the magnetic forces, that is, the magnetic Reynolds number is assumed small,

$$Re_M = \frac{Lu_0}{\eta} \ll 1 \tag{3}$$

where u_0 is the velocity of the moving boundary and the Hartmann number (2) is large. The above assumption of small Re_M implies that the flow-induced component of the magnetic field is of the order Re_M, and thus the magnetic field is decomposed in the following way

$$\mathbf{B} = \mathbf{B_0}(x,z) + Re_M b(x,z)\widehat{\mathbf{e}}_y \quad \text{for the plannar case} \tag{4}$$

$$\mathbf{B} = \mathbf{B_0}(s,z) + Re_M b(s,z)\widehat{\mathbf{e}}_\varphi \quad \text{for the spherical case} \tag{5}$$

where (s,φ,z) are the cylindrical polar coordinates, $\mathbf{B_0}$ is the external potential field, and $Re_M\mathbf{b}$ is the perturbation magnetic field generated by the flow. Indeed, in the numerical simulations of Hollerbach and Skinner [16] for infinitesimally small rotation rate, the flow was axisymmetric with only the azimuthal components of the velocity and the induced magnetic field present. The assumption of the small magnetic Reynolds number is crucial for the spherical case to neglect the nonlinear term which does not vanish because of the curvature effects. In the flat case, however, this assumption is not necessary to simplify the equations, because the nonlinear term vanishes due to the translational symmetry in the direction of the flow. Nevertheless, we keep the Reynolds numbers small even in the plane flow, since for high Rm, the unidirectional solutions are most probably unstable.

Furthermore, the solution for the plane flow is also valid when both boundaries are moving with different velocities since it is just a matter of changing the frame of reference to one moving at the same constant velocity as one of the boundaries. In the spherical case, however, when both boundaries rotate at different angular velocities, the Coriolis force substantially modifies the solution even in the case of small differential rotation unless the flow is strongly dominated by the magnetic force. The problem of MHD Couette flow with Coriolis force was investigated numerically by Hollerbach [17] and Dormy et al. [1] and analytically, for small Elsasser numbers, by N. Kleeorin et al. [18]. As remarked in the introduction, Brito et al. [8] demonstrated experimentally the detrimental effect of the Coriolis force on superrotation.

2.1. The equations and the main flow solution

As mentioned, we present the analysis for the flat case illustrated on the left panel of **Figure 1**. In Cartesian coordinates (x, y, z), the lower boundary is moving in the "y" direction and the "z" axis is perpendicular to both parallel boundaries. The dimensionless external magnetic field is given by

$$\mathbf{B_0}(x,z) = \nabla A \times \widehat{\mathbf{e}}_y = \nabla\Phi = \left[e^{-\lambda z}\sin\lambda x, 0, e^{-\lambda z}\cos\lambda x\right], \tag{6}$$

where $A = \exp(-\lambda z)\sin\lambda x/\lambda$, $\Phi = -\exp(-\lambda z)\cos\lambda x/\lambda$, and $2\pi/\lambda$ is the arbitrary period of oscillation of the external field in the "x" direction.

The lower moving boundary is assumed to have the same conductivity as the fluid, while the conductivity of the upper one, which is at rest,

$$\epsilon = \frac{\sigma_u}{\sigma_f} \tag{7}$$

can vary from zero to infinity, where σ_u and σ_f are the electrical conductivities of the upper boundary and the fluid, respectively. The magnetic permeabilities of boundaries and the fluid are assumed to be same.

The general set of equations for the analyzed stationary state is obtained by taking the "y" components of the induction and the Navier-Stokes equations

$$\begin{aligned} &\mathbf{B_0}\cdot\nabla u + \nabla^2 b = 0 \\ &\mathbf{B_0}\cdot\nabla b + \frac{1}{M^2}\nabla^2 u = 0 \end{aligned} \quad \text{for} \quad 0 < z < 1 \tag{8}$$

with $M \gg 1$ and no-slip boundary conditions for the velocity field $u(x,z)$

$$\begin{aligned} u(x,1) &= 0 \\ u(x,0) &= 1. \end{aligned} \tag{9}$$

Inside the rigid conductors, the magnetic field $\mathbf{b}$ has to satisfy Laplace equations:

$$\begin{aligned} \nabla^2 b_1 = 0 \quad &\text{for} \quad 1 < z < 1+\delta_1 \\ \nabla^2 b_2 = 0 \quad &\text{for} \quad -\delta_2 < z < 0 \end{aligned} \tag{10}$$

where b_i and δ_i are the perturbation magnetic fields inside the rigid conductors and their dimensionless thickness (with $i = 1$ for the upper conductor and $i = 2$ for the lower one). At the boundaries with the insulator at $z = 1 + \delta_1$ and at $z = -\delta_2$, the perturbation magnetic field must vanish since there is no imposed magnetic field in the "y" direction

$$\begin{aligned} b_1(x, 1+\delta_1) &= 0 \\ b_2(x, -\delta_2) &= 0 \end{aligned} \tag{11}$$

Finally, the conditions at $z = 0$ and at $z = 1$ for the magnetic field can be written in the following form

$$\begin{cases} b(x,0) = b_2(x,0) \\ \frac{\partial b}{\partial z}\big|_{z=0} = \frac{\partial b_2}{\partial z}\big|_{z=0} \end{cases} \text{ and } \begin{cases} b(x,1) = b_1(x,1) \\ \epsilon \frac{\partial b}{\partial z}\big|_{z=1} = \frac{\partial b_1}{\partial z}\big|_{z=1} \end{cases} \tag{12}$$

To understand the structure of the flow, it is very important to note the symmetries in the system with respect to planes defined by $x = n\frac{\pi}{2\lambda}$ for $n \in \mathbb{N}$ (see **Figure 1**). Since the problem has to be periodic in the "x" direction with the period of the applied field $\frac{2\pi}{\lambda}$, it is enough to analyze only the region where $0 < x < \frac{2\pi}{\lambda}$. The symmetry of the external field $\mathbf{B_0}$, the symmetric boundary conditions on $u(x,z)$, and the boundary conditions on $b(x,z)$ listed above imply that

$$\begin{cases} u\left(\frac{\pi}{2\lambda} - \alpha, z\right) = u\left(\frac{\pi}{2\lambda} + \alpha, z\right) \\ u\left(\frac{3\pi}{2\lambda} - \alpha, z\right) = u\left(\frac{3\pi}{2\lambda} + \alpha, z\right) \\ u\left(\frac{\pi}{\lambda} - \alpha, z\right) = u\left(\frac{\pi}{\lambda} + \alpha, z\right) \end{cases} \text{ and } \begin{cases} b\left(\frac{\pi}{2\lambda} - \alpha, z\right) = -b\left(\frac{\pi}{2\lambda} + \alpha, z\right) \\ b\left(\frac{3\pi}{2\lambda} - \alpha, z\right) = -b\left(\frac{3\pi}{2\lambda} + \alpha, z\right) \\ b\left(\frac{\pi}{\lambda} - \alpha, z\right) = b\left(\frac{\pi}{\lambda} + \alpha, z\right) \end{cases} \tag{13}$$

for any $\alpha \in \mathbb{R}$. One can see now the precise analogy between the flat and spherical cases. In the spherical problem, the meridional angle "ϑ" corresponds to the "x" coordinate in the flat case, with the equatorial plane corresponding to the planes $x = \frac{\pi}{2\lambda}$ and $x = \frac{3\pi}{2\lambda}$. The azimuthal angle "$\varphi$" and the radial coordinate "r" are of course analogous to "y" and "z," respectively.

It is also clear from (13) that the "z" component of the currents $j_z = \frac{\partial b}{\partial x}$ has to be symmetric with respect to the planes $x = \frac{\pi}{2\lambda}, \frac{3\pi}{2\lambda}$ while the "x" component $j_x = -\frac{\partial b}{\partial z}$ remains antisymmetric. This means that j_z must have an external value and j_x must vanish at $x = \frac{\pi}{2\lambda}, \frac{3\pi}{2\lambda}$.

The main flow is defined as the flow outside all boundary and internal layers in the problem. When the upper boundary is insulating or only weakly conducting, the problem is greatly simplified since the magnetic coupling of the fluid with the lower conductor, in the limit of the large Hartmann number, is much stronger than with the upper one. The fluid therefore should lock on to the lower boundary generating large shear in a Hartmann boundary layer adjacent to the upper conductor, where the velocity decreases to zero on a distance in the order of M^{-1}. This allows to deduce that the electrical currents in the system, generated by the flow and circulating through the boundary layers and both boundaries, in particular through the upper poor conductor, should scale as $O(M^{-1})$ everywhere except for the boundary layers where the shear is large. A schematic picture of the current circulation when the outer/upper boundary is poorly conducting or insulating for both geometries is provided in **Figure 3**. It follows, that everywhere the perturbation magnetic field is weak, that is $b(x,z) = O(M^{-1})$. Therefore, from (8), we infer that the main flow for the case of poorly conducting or insulating boundary is determined by

$$\begin{cases} \mathbf{B_o} \cdot \nabla u = 0 + O(M^{-1}) \\ \mathbf{B_o} \cdot \nabla b = 0 + O(M^{-2}) \end{cases} \Rightarrow \begin{cases} u = \mathcal{F}(A) + O(M^{-1}) \\ b = \mathcal{G}(A) + O(M^{-2}) \end{cases} \tag{14}$$

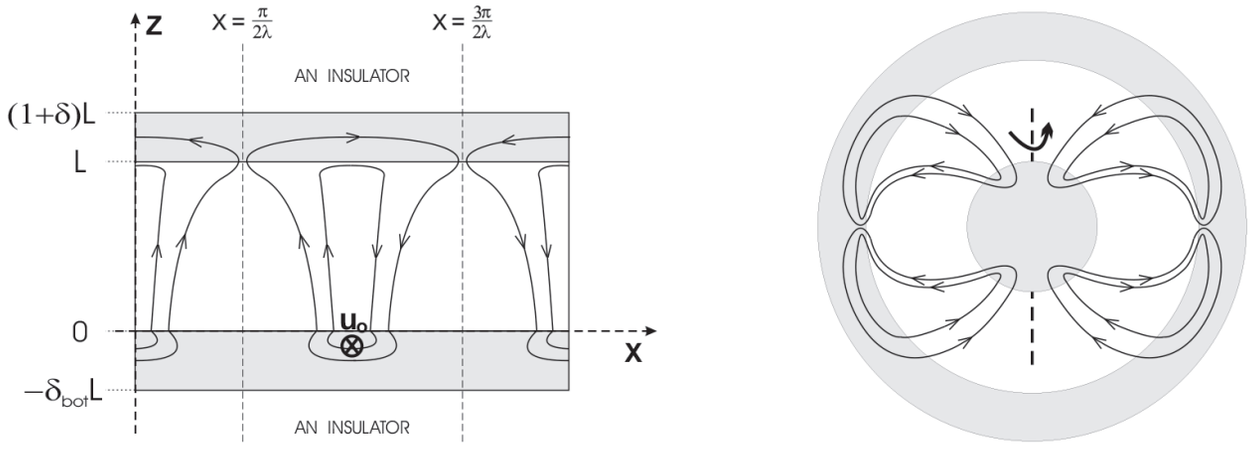

Figure 3. A schematic picture of the current circulation in the planar (left panel) and spherical (right panel) configurations. In the planar case, the direction of the external field oscillates in the x direction and so does the direction of currents, which are strongest in a shear layer along the critical $\mathcal{C}$-line. In the spherical case, strong currents flow from the inner sphere to the outer shell in the shear layer along $\mathcal{C}$ and return in polar regions.

where $\mathcal{F}$ and $\mathcal{G}$ depend on A alone, thus the flow and the induced magnetic field are constant on the field lines. The second equation in (14) means of course, that at the leading order, the Lorentz force vanishes everywhere in the main flow, which in turn implies that the currents are parallel to the external field $\mathbf{B_0}$.

It is clear now that the magnetic field lines which are tangent to the upper boundary, referred to as the $\mathcal{C}$ lines, divide the flow into three regions **I**, **II**, and **III** (see **Figure 1**), and the properties of the solution for each region are somewhat different since in regions **II** and **III**, the external field lines intersect with both boundaries and in region **I**, only with the lower one. Regions **II** and **III** are, therefore, very similar and the only difference between them is the sign of the perturbation magnetic field since it is antisymmetric with respect to the planes $x = \frac{\pi}{2\lambda}, \frac{3\pi}{2\lambda}$. This antisymmetry of b and symmetry of u, together with (14) results in

$$\begin{cases} u \equiv 1 + O\left(M^{-1}\right) \\ b \equiv 0 + O\left(M^{-2}\right) \end{cases} \text{ in region } \mathbf{I} \tag{15}$$

thus, the fluid in region **I** flows with the same uniform velocity of the bottom boundary and the perturbation magnetic field vanishes at leading order. Therefore, in region **I**, the currents also must vanish. However, in the area of singularity of the Hartmann layer, namely at $x = \frac{\pi}{2\lambda}, \frac{3\pi}{2\lambda}$ and at $z = 1$, the "z" component of the currents, as it was stated earlier, has an external value (while the "x" component is zero) and interacting with the external magnetic field creates a Lorentz force which has to either accelerate or decelerate the fluid depending on whether the signs of j_z and B_{0x} are the same or opposite.

Since the $\mathcal{C}$ lines that create the singularity of the upper Hartmann layer connect regions of different flow characteristics, a thin area along the lines has to be treated differently and the dissipation must play an important role in this region. Those are shear layers, for which the precise analysis allows to compute the magnitude of super velocity.

The situation is more complicated when the upper boundary is strongly conducting. According to Soward and Dormy [6], the Ferraro's law still holds in region **I** (equatorial region $\mathcal{E}$ for the spherical case) where the fluid locks on to the moving boundary, however, in regions **II** and **III** (equivalently in polar regions $\mathscr{P}$), the Ferraro's law is violated by the influence of ohmic diffusion. This happens, because the induced magnetic field b is no longer small, but of comparable magnitude with the velocity field. Nevertheless, the shear layer along the critical $\mathcal{C}$-line still forms and strong currents enter the upper boundary in the region of tangent contact between the line $\mathcal{C}$ and the boundary, thus creating strong Lorentz force, which accelerates the flow. The results of numerical simulations of Mizerski and Bajer [5] are recalled here on **Figure 4** to demonstrate the enhancement of super velocities with the increasing conductivity of the upper boundary.

The obvious conclusion of the above analysis is that the acceleration of the fluid at $x = \pi/2\lambda$ and $z \approx 1$ is due to the curvature of the applied field $\mathbf{B_0}$ generating singularity at this point, and the antisymmetry of external field's "z" component with respect to the plane $x = \pi/2\lambda$ which is responsible for the direction of the currents and therefore also the Lorentz force at $z = 1$. At the singular point, the intensity of the currents entering the boundary layer and the upper boundary increases with the conductivity of this boundary because its interaction with the conducting fluid strengthens. This also implies the increase of the magnitude of the super velocities with ϵ.

These conclusions are also true for the spherical case for which the whole analysis differs only with slightly more complicated boundary conditions and diffusive terms. This complication, however, at the leading order affects mainly the analysis of the shear layer presented in the next section but does not make the main flow analysis more difficult in any way.

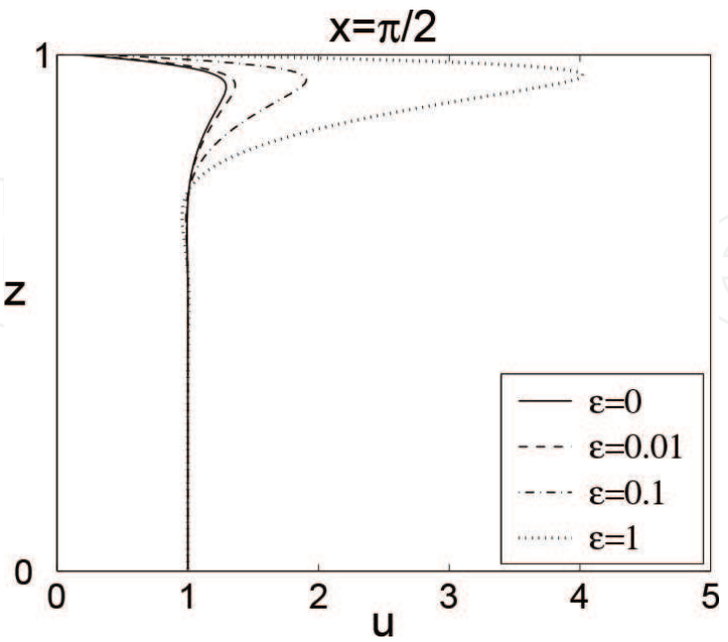

Figure 4. Velocity profiles at $x = \pi/2$ for four different values of the conductivity ratio for the upper boundary $\epsilon = 0$, 0.01, 0.1, and 1. The magnitude of super velocities is the highest near the upper boundary (in the region of singularity of the Hartmann layer) and significantly increases with ϵ. After Mizerski and Bajer [5].

It may also be interesting to make a comment on a similar problem studied numerically by Hollerbach & Skinner [16] of spherical Couette flow with axial magnetic field aligned with the axis of rotation in terms of the singular perturbation method for large Hartmann numbers, infinitesimal rotation and conductivity of the inner sphere. In this case, the Hartmann layers also become singular at the equator where the external filed becomes tangent to the boundaries. This time, however, only the singularity at the inner sphere is important since the field lines tangent to the outer shell leave the fluid and do not couple it to the boundary. Outside a cylinder tangent to the inner sphere and aligned with the axis of rotation the fluid must be at rest, since the velocity field must be constant on the magnetic field lines and the outer stationary sphere has the same conductivity as the fluid, thus the fluid is locked on to it. In such a case, the currents leaving the inner boundary layer at $\vartheta = \frac{\pi}{2}$ and interacting with the external magnetic field create a Lorentz force which decelerates the fluid and produce a counter-rotating jet as found by Hollerbach and Skinner [16].

A simple conclusion which can be stated now is that super- and counter-rotating jets in such MHD systems as considered above are, in general, the outcome of three major features of these systems: the presence of isolated singular points where the external magnetic field is tangent to the boundary, the symmetries of the external magnetic field in respect to planes containing the singular points and perpendicular to the boundaries (namely, antisymmetry of the component perpendicular to the boundary and symmetry of the parallel component) and the symmetric boundary conditions for the velocity field. However, as observed by [10] the singular points can also be created in side the domain (away from the boundaries) by a magnetic field configuration with X-type null points (see field configuration 4 in [10]); also in this case the presence of super-rotation depends on the conductivity of boundaries.

3. The shear layer along the $\mathcal{C}$-line

We will now briefly introduce the reader into the mathematical approach to the analysis of the shear layer structure, which is based on the singular perturbation theory. To take into account of the curvature of the $\mathcal{C}$-line, it is more suitable to use different variables. As mentioned, the symmetries of the system imply that it is enough to limit the analysis to the interval $0 < x < \pi/2\lambda$. Thus, the magnetic field lines can be represented parametrically in the following way

$$\begin{aligned} x(\tau) &= \lambda A(\tau - 1) + \frac{\pi}{2\lambda} \\ \exp[\lambda z(\tau)] &= \frac{1}{\lambda A}\sin\left[\lambda^2 A(\tau - 1) + \frac{\pi}{2}\right] \end{aligned} \tag{16}$$

and the point $x = \frac{\pi}{2\lambda}$, $z = 1$ where the Hartman layer singularity occurs (referred to as the point $\mathcal{S}$ (see **Figure 5**)) is defined by $A = A_{\mathcal{C}}$ and $\tau = 1$. Introducing a measure of distance along the critical $\mathcal{C}$-line

$$\gamma(\tau) = -\int_{\mathcal{S}} \mathbf{B}\cdot\mathbf{dr} = -\int_{\mathcal{S}} d\Phi = \frac{e^{-\lambda z(\tau')}}{\lambda}\cos[\lambda x(\tau')]\Big|_1^{\tau} = -A\tan\left[\lambda^2 A(\tau - 1)\right], \tag{17}$$

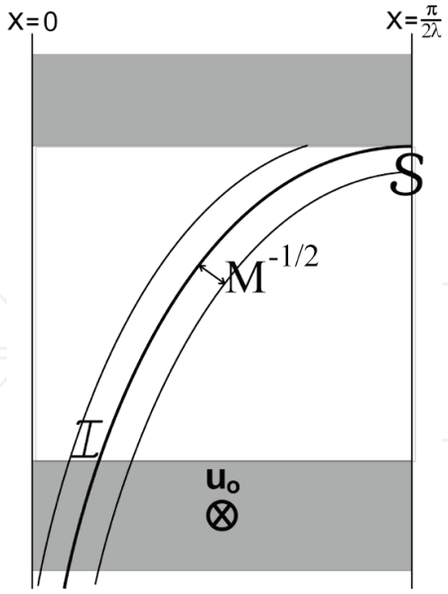

Figure 5. The shear layer along the critical magnetic field line $\mathcal{C}$. The point $\mathcal{S}$ is the point $x = \frac{\pi}{2\lambda}$, $z = 1$ at which the line grazes the upper boundary and the point of intersection of the critical line with the lower boundary is denoted by $\mathcal{I}$. After Mizerski and Bajer [5].

and letting $\Gamma = \gamma(\tau_{\mathcal{I}})$ be the distance between point $\mathcal{S}$ and the point of intersection of the field line $\mathcal{C}$ with the lower boundary (referred to as the point $\mathcal{I}$ (see **Figure 5**)) we introduce a new set of coordinates

$$l = 1 - \frac{\gamma(\tau)}{\Gamma} = 1 - \frac{e^{-\lambda z}}{\lambda\Gamma}\cos(\lambda x) \tag{18}$$

$$n = M^{\frac{1}{2}}\sqrt{\Gamma}(A_{\mathcal{C}} - A) = M^{\frac{1}{2}}\sqrt{\Gamma}\left(A_{\mathcal{C}} - \frac{e^{-\lambda z}}{\lambda}\sin(\lambda x)\right) \tag{19}$$

where l is the coordinate along the basic magnetic field lines which has the property that $l = 1$ at $\mathcal{S}$ and $l = 0$ at $\mathcal{I}$, whereas n is a measure of distance between other field lines and the $\mathcal{C}$-line within the shear layer of thickness $M^{-1/2}$ (cf. [19, 20]). The so-defined coordinate n has the properties, that it is 0 on the $\mathcal{C}$-line, positive in region **II** and negative in region **I**; moreover $A_{\mathcal{C}} = \exp(-\lambda)/\lambda = \sqrt{1 - \lambda^2\Gamma^2}/\lambda$.

For the simplest case of poorly conducting or insulating upper/outer boundary, with the use of the shear layer coordinates (l, n), the Eq. (8) can now be written at the leading order in the form

$$\frac{\partial V_{\pm}}{\partial l} \pm \frac{\partial^2 V_{\pm}}{\partial n^2} = 0 \tag{20}$$

where

$$V_{\pm} = u \pm Mb. \tag{21}$$

In the spherical geometry, the analogous formulation leads to the coupling of the two equations for $V_{\pm}$ through nonzero curvature terms on the right-hand sides

$$\frac{\partial V_{\pm}}{\partial l} \pm \frac{\partial^2 V_{\pm}}{\partial n^2} = \frac{1}{s_c}\frac{\mathrm{d}s_c}{\mathrm{d}l} V_{\mp}. \tag{22}$$

The coupling term, however, may be neglected if the narrow gap limit is assumed. More importantly, however, the two equations, in both—planar and spherical configurations, are coupled through the boundary conditions at $l = 0, 1$, thus at the points $\mathcal{I}$ and $\mathcal{S}$. Eqs. (20) and (22) are diffusion equations (with a source in the spherical case) valid for all $\infty < n < \infty$, with the variable l corresponding to time variable from standard diffusion processes in the case of V_- and $1 - l$ corresponding to time in the case of V_+. The following solving procedure of Eqs. (20) or (22) can be applied. One can utilize the Green's formula for the diffusion equation and first solve for V_+ by the use of the "initial condition" at $l = 1$ $(1 - l = 0)$. Then introduce the obtained expression for V_+ into the "initial condition" for V_- at $l = 0$ and utilize the Green's formula again. Finally, matching the two solutions through the condition at $l = 1$ again yields an integral equation for the super velocities. Such procedure leads to an integral equation of Fredholm type, which has been solved numerically in Dormy et al. [4] and Mizerski and Bajer [5] for the two cases $\epsilon = 0$ and $\epsilon = M^{-1}$.

However, when the boundaries are perfectly conducting, the problem becomes more complicated. The same equations as (20) and (22) are obtained for

$$V_{\pm} = M^{-1/2}u \pm M^{1/2}b. \tag{23}$$

(cf. Eq. (3.20) in [6]), but the problem becomes analytically intractable due to the complications arising from vanishing of the current component parallel to the boundary at $l = 1$. Nevertheless, Soward and Dormy [6] have managed to show that for perfectly conducting boundaries, the strong current leakage from the shear layer into the outer boundary in the vicinity of the critical point causes strong super rotation $\Omega = \mathcal{O}\left(M^{1/2}\right)$.

4. Summary

The plane and spherical magnetohydrodynamic Couette flow with an applied strong external magnetic field creating Hartmann layer singularities on a boundary is a setting where fastly moving jets form, with the magnitude of the flow exceeding that of the moving boundary, which drives the entire flow. These are the so-called super velocities (super rotation in the spherical case). We have concentrated here on the review of the results and analytic approach to the problem of the formation of super velocities in strong, potential fields, with particular emphasis on the enhancement of super velocities by the conductivity of the resting boundary.

As found by Soward and Dormy [6], the conductivity of the resting (upper/outer) boundary ε greatly influences the current leakage from the shear layer to that boundary near the point of its tangent contact with the critical $\mathcal{C}$-line. In the case of weakly conducting boundary $\epsilon M^{3/4} \ll 1$, the current leakage is of the order $\mathcal{O}\left(\epsilon M^{3/4}\right)$ and it increases with ε to become order unity when $\epsilon M^{3/4} \gg 1$. This strong current is perpendicular to the external field in the

singular region, and thus a strong Lorentz force $\mathbf{j} \times \mathbf{B}_0$ is created, which accelerates the flow (or decelerates in some cases as shown by [16], depending on the symmetries of the applied field). In the case of interest when the moving boundary is strongly conducting and $M \gg 1$, the resulting super-velocity scales like $\mathcal{O}\left(M^{1/2}\right)$ when $\epsilon \gg 1$ is of the order $\mathcal{O}\left(\epsilon^{2/3} M^{1/2}\right)$ when $1 \gg \epsilon \gg M^{-3/4}$ and becomes order unity when $\epsilon \ll M^{-3/4}$.

Author details

Krzysztof Mizerski

Address all correspondence to: kamiz@igf.edu.pl

Institute of Geophysics, Polish Academy of Sciences, Warsaw, Poland

References

[1] Dormy E, Cardin P, Jault D. MHD flow in a slightly differentially rotating spherical shell, with conducting inner core, in a dipolar magnetic field. Earth and Planetary Science Letters. 1998;**160**:15-30

[2] Hollerbach R. Magnetohydrodynamic flows in spherical shells. In: Egbers C, Pfister G, editors. Physics of Rotating Fluids. Vol. 549. Lecture Notes in Physics. Berlin, Germany: Springer; 2000. pp. 295-316

[3] Hollerbach R. Super- and counter-rotating jets and vortices in strongly magnetic spherical Couette flow. In: Chossat P, Armbruster D, Oprea I, editors. Dynamo and Dynamics, A Mathematical Challenge. Vol. 26. NATO Science Series II. Dordrecht: Kluwer; 2001. pp. 189-197

[4] Dormy E, Jault D, Soward AM. A super-rotating shear layer in magnetohydrodynamic spherical Couette flow. Journal of Fluid Mechanics. 2002;**452**:263-291

[5] Mizerski KA, Bajer K. On the effect of mantle conductivity on super-rotating jets near the liquid core surface. Physics of the Earth and Planetary Interiors. 2007;**160**:245-268

[6] Soward AM, Dormy E. Shear layers in magnetohydrodynamic spherical Couette flow with conducting walls. Journal of Fluid Mechanics. 2010;**645**:145-185

[7] Nataf H-C, Alboussière T, Brito D, Cardin P, Gagnière N, Jault D, Masson J-P, Schmitt D. Experimental study of super-rotation in a magnetostrophic spherical Couette flow, Geophysical and Astrophysical Fluid Dynamics. 2006;**100**:281-298

[8] Brito D, Alboussière T, Cardin P, Gagnière N, Jault D, La Rizza P, Masson J-P, Nataf H-C, Schmitt D. Zonal shear and super-rotation in a magnetized spherical Couette-flow experiment. Physical Review E. 2011;**83**:066310

[9] Wei X, Hollerbach R. Magnetic spherical Couette flow in linear combinations of axial and dipolar fields. Acta Mechanica. 2010;**215**:1-8

[10] Hollerbach R, Hulot D. Shercliff layers in strongly magnetic cylindrical Taylor-Couette flow. Comptes Rendus Mécanique. 2016;**344**:502-509

[11] Song X, Richards PG. Seismological evidence for differential rotation of the Earth's inner core. Nature. 1996;**382**:221-224

[12] Su W, Dziewonski AM, Jeanloz R. Planet within a planet: Rotation of the inner core of earth. Science. 1996;**274**:1883-1887

[13] Alexandrescu M, Gibert D, Le Mouël J-L, Hulot G, Saracco G. An estimate of average lower mantle conductivity by wavelet analysis of geomagnetic jerks. Journal of Geophysical Research. 1999;**104**(B8):17735-17745

[14] Dubrovinsky L, Dubrovinskaia N, Langenhorst F, Dobson D, Rubie D, Geβmann C, Abrikosov IA, Johansson B, Baykov VI, Vitos L, Le Bihan T, Crichton WA, Dmitriev V, Weber H-P. Iron-silica interaction at extreme conditions and the electrically conducting layer at the base of Earth's mantle. Nature. 2003;**422**:58-61

[15] Holme R. Electromagnetic core – mantle coupling – I. Explaining decadal changes in the length of day. Geophysical Journal International. 1998;**132**:167-180

[16] Hollerbach R, Skinner S. Instabilities of magnetically induced shear layers and jets. Proceedings of the Royal Society of London A. 2001;**457**:785-802

[17] Hollerbach R. Magnetohydrodynamic Ekman and Stewartson layers in a rotating spherical shell. Proceedings of the Royal Society of London A. 1994;**444**:333-346

[18] Kleeorin N, Rogachevskii L, Ruzmaikin A, Soward AM, Starchenko S. Axisymetric flow between diferentially rotating spheres in a dipole magnetic field. Journal of Fluid Mechanics. 1997;**344**:213-244

[19] Starchenko SV. Magnetohydrodynamic flow between insulating shells rotating in strong potential field. Physics of Fluids. 1998;**10**:2412-2420

[20] Starchenko SV. Strong potential field influence on slightly differentially rotating spherical shells. Studia Geophysica et Geodaetica. 1998;**42**:314-319

IntechOpen